

Iodide and Triiodide Anion Complexes Involving Anion- π Interactions with a Tetrazine-based Receptor

Received 00th January 20xx,
Accepted 00th January 20xx

DOI: 10.1039/x0xx00000x

www.rsc.org/

Matteo Savastano,^a Carla Bazzicalupi,^a Celeste García,^b Cristina Gellini,^a Maria Dolores López de la Torre,^b Palma Mariani,^a Fabio Pichierri,^c Antonio Bianchi,^{*a} Manuel Melguizo^{*b}

Protonated forms of the tetrazine ligand L2 (3,6-bis(morpholin-4-ylethyl)-1,2,4,5-tetrazine) interact with iodide in aqueous solution forming relatively stable complexes ($\Delta G^\circ = -11.6(4)$ kJ/mol for $\text{HL2}^+ + \text{I}^- = (\text{HL2})\text{I}$ and $\Delta G^\circ = -13.4(2)$ kJ/mol for $\text{H}_2\text{L2}^{2+} + \text{I}^- = [(\text{H}_2\text{L2})\text{I}]^+$). When solutions of $[(\text{H}_2\text{L2})\text{I}]^+$ are left in contact with the air, crystals of the oxidation product $(\text{H}_2\text{L2})_2(\text{I}_3)_3 \cdot 4\text{H}_2\text{O}$ are formed. Unfortunately, the low solubility of I_3^- complexes prevents the determination of their stability constants. The crystal structures of $\text{H}_2\text{L2I}_2 \cdot \text{H}_2\text{O}$ (**1**), $\text{H}_2\text{L2}(\text{I}_3)_2 \cdot 2\text{H}_2\text{O}$ (**2**) and $(\text{H}_2\text{L2})_2(\text{I}_3)_3 \cdot 4\text{H}_2\text{O}$ (**3**) were determined by means of X-ray diffraction analyses. In all crystal structures, it was found that the interaction between I^- and I_3^- with $\text{H}_2\text{L2}^{2+}$ is dominated by anion interactions with the π electron density of the receptor. Only in the case of **1**, the iodide anions involved in close anion- π interactions with the ligand tetrazine ring form an additional H-bond with the protonated morpholine nitrogen of an adjacent ligand molecule. Conversely, in crystals of **2** and in **3** there are alternated segregated planes which contain only protonated ligands hydrogen-bonded to cocrystallized water molecules or I_3^- and I^- forming infinite two-dimensional networks established through short interhalogen contacts, making these crystalline products good candidates to behave as solid conductors. In the solid complexes, the triiodide anion displays both end-on and side-on interaction modes with the tetrazine ring, in agreement with density functional theory calculations indicating a preference for the alignment of the I_3^- molecular axis with the molecular axis of the ligand. Further information about geometries and structures of triiodide anions in **2** and **3** were acquired by the analysis of their Raman spectra.

Introduction

Anion binding has earned much attention because of the crucial role played by anionic species in biological and chemical systems.¹ As with all areas of supramolecular chemistry, anion binding is governed by weak forces, mostly electrostatic attraction, hydrogen bonding and/or hydrophobic effects. Nevertheless, also the weak attractive forces exerted between anions and the π -system of electron-deficient arenes, the so called anion- π interactions, have gained increasing consideration in recent years^{2,3} and are now included among the most appealing forces for the make-up of new functional materials,⁴ anion receptors,^{3a,5} carriers⁶ and catalysts,⁷ while their biological relevance^{3a,b} is increasingly valued.

Within the multifaceted chemistry of anions, the behaviour of iodide and polyiodides occupies a special position, as a wide spectrum of structures, ranging from isolated units to complicated three-dimensional networks, passing through linear chains and two-dimensional assemblies, can be generated from three simple building blocks: I_2 , I^- and I_3^- . This kind of structural features are made possible by the ability of iodine to concatenate *via* donor-acceptor interactions, the character of each assembly being regulated by its chemical environment.⁸ In the solid state, for instance, polyiodides of

variable structures can be generated by using different counteranions.⁹

The understanding of such a structural variety is an interesting challenge, especially when considering that the hypervalency exhibited by several large polyiodides is not easily justified by simple covalent bonding models and, accordingly, the nature of bonding in polyiodide anions has been the object of intense theoretical consideration.¹⁰ Furthermore, the particular electrical conductivity¹¹⁻¹³ and redox properties of polyiodide systems have grown interest toward their application for the development of dye-sensitized solar cells¹⁴ and solar batteries,¹⁵ where they have been incorporated in many different forms, including aqueous solutions,^{16,17} ionic liquid electrolytes,¹⁸ gel polymer electrolytes^{14a,19-21} or even solid state crystalline conductors (refs. 22-25).

We have recently reported that ligands L1 and L2, constituted by a tetrazine ring decorated with two morpholine pendants of different lengths (Fig. 1), are able to form stable anion complexes in solution. All crystal structures we obtained for such complexes (PF_6^- and ClO_4^- complexes with $\text{H}_2\text{L1}^{2+}$ and NO_3^- , PF_6^- and ClO_4^- complexes with $\text{H}_2\text{L2}^{2+}$) invariably showed that the anions are involved in anion- π interactions with the tetrazine group, in agreement with the strong π -acid character of this ring.²⁵ These results encouraged us to further investigate the anion binding ability of these ligands, and the iodide/polyiodides system seemed an intriguing medium to explore new effects of these anion receptors molecules. Unfortunately, it was not possible to test L1 toward this anionic system, as it undergoes rapid degradation in the presence of I^- , even in slightly acidic media, but as shown in the following, protonated forms of L2 do interact with I^- in aqueous solution, from which the crystalline iodide complex $\text{H}_2\text{L2I}_2 \cdot \text{H}_2\text{O}$ (**1**) can be isolated, and depending on the medium

^a Department of Chemistry "Ugo Schiff", University of Florence, Via della Lastruccia 3, 50019, Sesto Fiorentino, Italy. E-mail: antonio.bianchi@unifi.it

^b Department of Inorganic and Organic Chemistry, University of Jaén 23071, Jaén, Spain. E-mail: mmelgui@ujaen.es

^c Department of Applied Chemistry, Graduate School of Engineering, Tohoku University, Sendai 980-8579, Japan. E-mail: fabio@che.tohoku.ac.jp

† Electronic Supplementary Information (ESI) available: Crystal packing of compound **1**. Superimposition of ligand and water molecules of the crystalline structures **2** and **3**. CCDC 1518137-1518139. For ESI and crystallographic data in CIF format see DOI: 10.1039/x0xx00000x

conditions, also the mixed iodide/triiodide $(\text{H}_2\text{L}_2)_2(\text{I}_3)_3 \cdot 4\text{H}_2\text{O}$ (**2**) and the triiodide $\text{H}_2\text{L}_2(\text{I}_3)_2 \cdot 2\text{H}_2\text{O}$ (**3**) complexes can be obtained. In these two later structures, it is remarkable the segregation of the anion iodine species into distinct layers that alternate with layers exclusively formed by protonated ligands and water molecules. All crystal structures of these complexes show that anion- π interactions with the tetrazine ring of L2 are widespread elements of such crystalline assemblies in which the anions show different binding modes and aggregation patterns.

Experimental procedures

Materials

L2 (3,6-bis(morpholin-4-ylethyl)-1,2,4,5-tetrazine) was synthesized as previously described.²⁵ Deep pink crystals of $\text{H}_2\text{L}_2 \cdot 2\text{H}_2\text{O}$ were obtained upon evaporation at room temperature, under nitrogen atmosphere, of an aqueous solution of L (0.01M) at pH 3 containing a fivefold excess of I^- . When maintained in contact with the mother liquor and exposed to the air, these crystals slowly re-dissolve while poorly soluble brownish orange crystals of $(\text{H}_2\text{L}_2)_2(\text{I}_3)_3 \cdot 4\text{H}_2\text{O}$ grow. Very insoluble dark brown crystals of $\text{H}_2\text{L}_2(\text{I}_3)_2 \cdot 2\text{H}_2\text{O}$ were prepared by slow diffusion, in a H-shaped tube, of initially separated aqueous solution of L2 and I_3^- at pH 3. Merck Suprapur grade NaI was used for the potentiometric measurement.

Potentiometric Measurements

Potentiometric (pH-metric) titrations employed for the determination of equilibrium constants were carried out in 0.1 M Me_4NCl degassed aqueous solutions at 298.1 ± 0.1 K by using previously described equipment and procedures.²⁶ The determined ionic product of water was $\text{p}K_w = 13.83(1)$ (298.1 ± 0.1 K, 0.1 M Me_4NCl). The computer program HYPERQUAD²⁷ was used to calculate equilibrium constants from potentiometric data deriving from three independent titration experiments. Ligand concentration was 5×10^{-4} M, while I^- concentration was 2.5×10^{-3} M. The studied pH range was 4.0-9.

X-ray Structure Analyses

Pink crystals of $\text{H}_2\text{L}_2 \cdot 2\text{H}_2\text{O}$ (**1**), dark orange crystals of $\text{H}_2\text{L}_2(\text{I}_3)_2 \cdot 2\text{H}_2\text{O}$ (**2**) and dark brown crystals of $(\text{H}_2\text{L}_2)_2(\text{I}_3)_3 \cdot 4\text{H}_2\text{O}$ (**3**) were used for X-ray diffraction analysis. A summary of the crystallographic data is reported in Table 1. The integrated intensities were corrected for Lorentz and polarization effects and an empirical absorption correction was applied.²⁸ The structures were solved by direct methods (SHELXS-86).²⁹ Refinements were performed by means of full-matrix least-squares using SHELX Version 2014/7 program.³⁰ All the non-hydrogen atoms were anisotropically refined. Hydrogen atoms were usually introduced in calculated position and their coordinates were refined according to the linked atoms, with the exception of the cocrystallized water molecules. In some cases, residual electron density remained at the end of

refinements close to iodine atoms most likely due to series truncation errors.

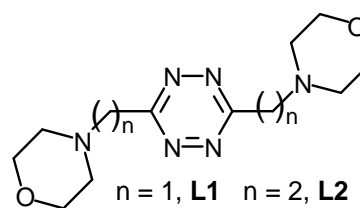


Fig. 1 The tetrazine ligands L1 and L2.

Table 1 Crystal data and structure refinement for $\text{H}_2\text{L}_2 \cdot 2\text{H}_2\text{O}$ (**1**), $\text{H}_2\text{L}_2(\text{I}_3)_2 \cdot 2\text{H}_2\text{O}$ (**2**) and $(\text{H}_2\text{L}_2)_2(\text{I}_3)_3 \cdot 4\text{H}_2\text{O}$ (**3**)

$$* R1 = \sum ||F_o| - |F_c|| / \sum |F_o| ; wR2 = [\sum w(F_o^2 - F_c^2)^2 / \sum wF_o^4]^{1/2}$$

	(1)	(2)	(3)
Empirical formula	$\text{C}_{14}\text{H}_{26}\text{I}_2\text{N}_6\text{O}_3$	$\text{C}_{14}\text{H}_{26}\text{I}_6\text{N}_6\text{O}_4$	$\text{C}_{14}\text{H}_{26}\text{I}_5\text{N}_6\text{O}_4$
Formula weight	580.21	1103.81	976.91
Temperature (K)	150	100	100
space group	<i>P</i> -1	<i>P</i> -1	<i>P</i> 2 ₁ /c
<i>a</i> (Å)	7.7303(6)	7.5053(6)	14.3403(3)
<i>b</i> (Å)	7.7864(6)	13.5410(7)	14.3161(2)
<i>c</i> (Å)	22.022(2)	14.5928(9)	13.8619(3)
α (°)	86.949(7)	99.590(5)	90
β (°)	87.158(7)	102.045(6)	106.228(2)
γ (°)	60.575(8)	94.974(5)	90
Volume (Å ³)	1152.5(2)	1418.74(16)	2732.42(9)
Z	2	2	4
Independent reflections / R(int)	3664 / 0.0450	4334 / 0.0986	5256 / 0.1171
μ (mm ⁻¹)	2.751/ (Mo- $\kappa\alpha$)	6.598/ (Mo- $\kappa\alpha$)	5.720/ (Mo- $\kappa\alpha$)
R indices [<i>I</i> >2 σ (<i>I</i>)]*	R1 = 0.0517 wR2 = 0.0628 R1 = 0.0857	R1 = 0.1013 wR2 = 0.2418 R1 = 0.1201	R1 = 0.0660 wR2 = 0.1706 R1 = 0.0927
R indices (all data)*		wR2 = 0.0793	wR2 = 0.2694 wR2 = 0.2053

Raman spectroscopy

The Raman spectra of **2** and **3** were recorded with a Bruker MultiRAM FT-Raman spectrometer equipped with a Nd-YAG laser emitting at 1064 nm as excitation source. The spectra were recorded on the pure compounds pressed in solid pellets with 4 cm⁻¹ slits, 100 mW power and acquiring for 1000 scans. Lower slit width gave only a worse signal-to-noise ratio without increasing the resolutions.

Computational chemistry

Density functional theory (DFT) calculations were performed with the Gaussian09 quantum chemistry package³¹ using the dispersion-corrected ω B97X-D functional of Chai and Gordon³² in combination with the all-electron DGDZVP basis set (ref. 33, 34). Geometry optimizations were carried out with the integral equation formalism-polarization continuum model (IEF-PCM) of Tomasi and coworkers³⁵ to simulate an implicit water environment surrounding the tetrazine-anion complexes. Binding energies (Be) for the tetrazine-anion complexes were

corrected for the basis-set superposition error (BSSE) using the counterpoise method of Boys and Bernardi.³⁶ Atom charges were obtained with a natural population analysis³⁷ of the solvated complexes. The topological analyses of the electronic charge densities of the complexes were carried out with the aid of the AIMAll software³⁸ which implements the theoretical concepts of Bader's quantum theory of atoms in molecules (QTAIM³⁹).

Results and discussion

In a previous paper we showed that the protonated HL2⁺ and H₂L2²⁺ forms and, in some cases, even the uncharged (not protonated) L2 ligand are able to bind anions, such as F⁻, NO₃⁻, PF₆⁻, ClO₄⁻, and SO₄²⁻, forming 1:1 anion-to-ligand complexes in aqueous solution.²⁵ Thermodynamic data obtained for these binding equilibria, in particular those concerning the formation of anion complexes with the uncharged ligand, suggested that anion- π interactions afford a prominent contributions to the interplay of weak forces stabilizing these complexes in solution, while crystallographic data exhibited the relevance of anion- π interactions in defining the relative position of the two interacting partners in the crystalline complexes. Also I⁻ forms 1:1 complexes with both HL2⁺ and H₂L2²⁺ but fails to interact, at least within the detection limits of the potentiometric measurements, with the neutral ligand. Similar results were obtained for the interaction with F⁻,²⁵ although this anion forms complexes of slightly lower stability than I⁻ (Table 2). These results might seem rather surprising, since F⁻ has a greater charge density and a greater propensity to form hydrogen bonds than I⁻, but they actually are in line with previous evidences that electrostatic attraction and hydrogen bonding are not the principal forces pushing together the partners of the anion complexes formed by this ligand,²⁵ although such forces appear to be of utmost importance in promoting the formation of anion complexes with most of ammonium receptors.⁴⁰ Accordingly, also in the case of I⁻, complex stability is poorly correlated with ligand charge, the binding free energy increasing by only 1.8 kJ/mol from HL⁺ to H₂L²⁺ (Table 2). It was previously inferred that solvation effects, principally involving the ligand, afford a significant contribution to the stability of such anion complexes.²⁵ Anion solvation, on the other side, could make the difference in determining the binding energy of different anions. In the particular case of I⁻ and F⁻ complexes with L2, the considerably lower hydration free energy of the former is expected to make an important contribution to the greater stability of its complexes.

Table 2 Equilibrium constants and relevant $-\Delta G^\circ$ values for anion complex formation determined at 298.1±0.1 K in 0.1 M Me4NCl aqueous solution.

	log K	$-\Delta G^\circ$ (kJ/mol)
HL2 ⁺ + I ⁻ = (HL2)I	2.03(7) ^a	11.6(4)
H ₂ L2 ²⁺ + I ⁻ = [(H ₂ L2)I] ⁺	2.35(4)	13.4(2)
HL2 ⁺ + F ⁻ = (HL2)F	1.58(8) ^b	9.0(5) ^b
H ₂ L2 ²⁺ + F ⁻ = [(H ₂ L2)F] ⁺	1.97(3) ^b	11.2(2) ^b

^a Values in parentheses are standard deviation on the last significant figure. ^b Taken from ref. 25.

Crystals of (H₂L2)₂I₂·H₂O (**1**) suitable for single crystal X-ray analysis were obtained by slow evaporation of an aqueous solution containing L and I⁻ at pH 3, in an anaerobic atmosphere at room temperature. Microcrystalline samples of the same compound can be obtained even under aerobic conditions provided that crystallization occurs in a few hours, otherwise complex (H₂L2)₂(I₃)₃·4H₂O (**3**) is obtained. The crystal packing of **1** is built up by alternate planes of two sets of symmetry independent H₂L2I₂ adducts developing in the (001) and the (002) crystallographic planes, respectively. In each H₂L2I₂ adduct (Fig. 2 and 3), the ligand is placed around an inversion centre, giving rise to anion- π interactions with two iodide anions placed one above and one below its tetrazine ring (I \cdots ring centroid /offset distances 3.70 /0.32 Å – (001) plane– and 3.67/0.27 Å –(002) plane–). Moreover, each iodide is H-bonded to two adjacent ligand molecules, through the protonated morpholine nitrogen on one side and a CH hydrogen bond on the other one (N \cdots I 3.451(8) Å and C \cdots I 4.010(8) Å –(001) plane, Fig. 2b– and N \cdots I 3.485(6) Å and C \cdots I 4.046(3) Å –(002) plane Fig. 3b–). In the (001) plane, the NH \cdots I contacts are directed along the *b* axis, while, in the (002) plane, the analogous contacts point in the [100] direction. Actually, both ligand conformations and relative anion/receptor spatial dispositions are very similar, and the major reason for the lack of additional crystallographic symmetries is the presence of a co-crystallized water molecule which joins the two H₂L2I₂ systems, forming stronger interactions with the one developing in the (002) plane (OW1 \cdots C9 3.68(1) Å, Fig. S1†).

In both planes, the conformation assumed by the ligand can be considered intermediate between the planar and the chair conformations previously observed in the crystal structures of H₂L2²⁺ complexes with ClO₄⁻, PF₆⁻ and NO₃⁻ anions.²⁵ Interestingly, in most of these complexes, as well as in all crystal structures solved up to now for the anion complexes with L1, anion and receptor almost exclusively form anion- π contacts, without the contribution of additional H-bonds from

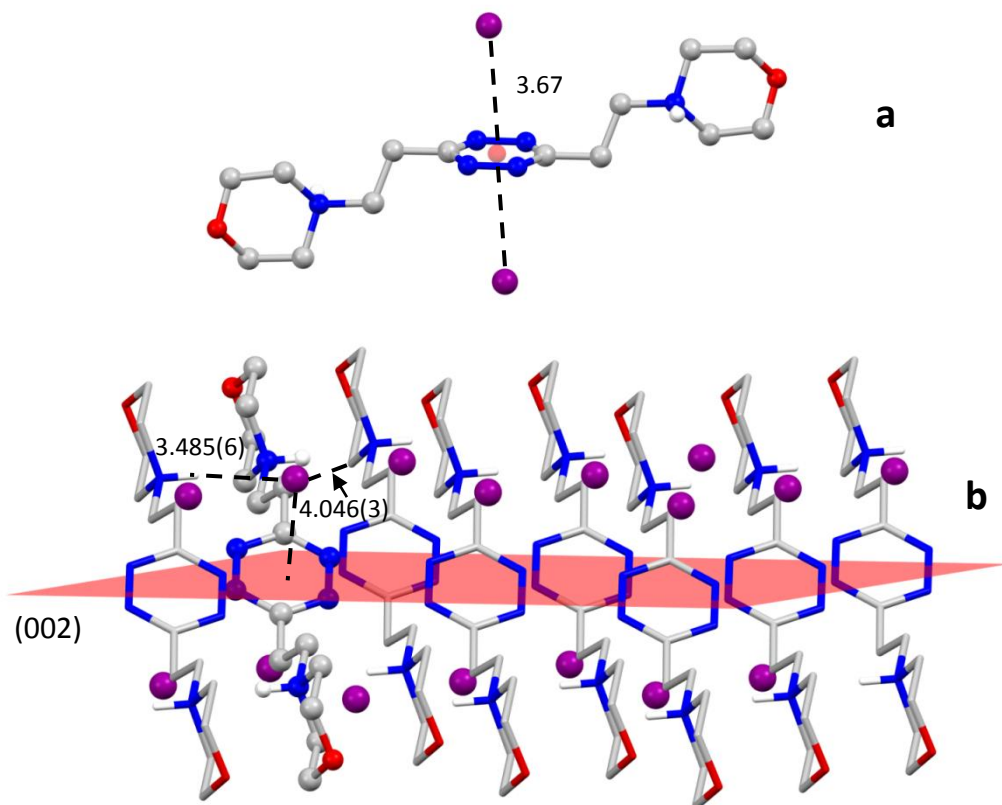


Fig. 2 Crystal structure of $(\text{H}_2\text{L}2)_2 \cdot \text{H}_2\text{O}$ (1): ligand conformation and anion... π contacts (a) in $\text{H}_2\text{L}2$ adduct developing in the (001) crystallographic plane (b). Distances are in Å.

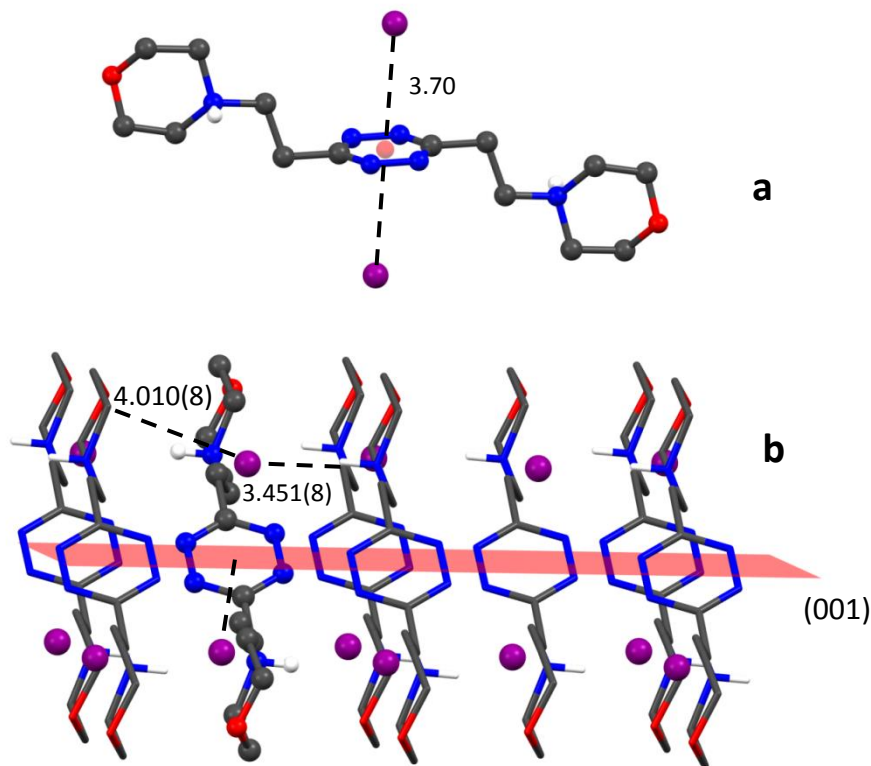


Fig. 3 Crystal structure of $(\text{H}_2\text{L}2)_2 \cdot \text{H}_2\text{O}$ (1): ligand conformation and anion... π contacts (a) in $\text{H}_2\text{L}2$ adduct developing in the (002) crystallographic plane (b). Distances are in Å.

the protonated nitrogen atoms, which, instead, are very often in contact with water solvent molecules.

In analogy with the behaviour seen in these structures, we can hypothesize that, even in $\text{H}_2\text{L}_2\text{I}_2$, the anion- π interaction strongly contributes to stabilize the complex. As a matter of fact, the anion is very well placed above the ring centroid, and the anion...centroid distance (3.67 and 3.70 Å) is significantly short with respect to the iodide ionic radius (2.20 Å).

When crystals of **1** are left in contact with the mother liquor and exposed to the air, they slowly re-dissolve while crystals of $(\text{H}_2\text{L}_2)_2(\text{I}_3)_3 \cdot 4\text{H}_2\text{O}$ (**3**) are formed as a consequence of the spontaneous air oxidation of I^- to I_2 (I_3^-). Crystals of **3** are also the product of slow evaporation of acidic solutions of L2, not protected from the air, in the presence of I^- . No further air oxidation of this compound was observed over several months. The very insoluble $\text{H}_2\text{L}_2(\text{I}_3)_2 \cdot 2\text{H}_2\text{O}$ (**2**) complex was obtained from the components by using a diffusion method (see the experimental section).

The crystal structures of **2** and **3** show close analogies, despite crystals of these complexes belong to different space groups and crystal systems (Table 1). In the case of **2**, the asymmetric unit contains two half ligand molecules, each interacting with triiodide through the tetrazine ring. In particular, as shown in Fig. 4a,b, both end-on (a) and side-on (b) binding modes are found. In the case of triiodide (a), the I...ring centroid distance is 3.60 Å with an offset of 0.45 Å. This triiodide is almost symmetric and linear (I-I 2.94(2) and 2.91(2) Å, I-I-I angle 178.28(6)°). Instead, the anion (b) is strongly asymmetric, bent (I-I 2.796(2) and 3.098(2) Å, I-I-I angle 174.25(6)°) and almost

aligned along the C-C axis. The central iodine atom is almost perfectly placed above a tetrazine nitrogen. The I...N distance is only 3.64(2) Å, significantly shorter than the sum of the van der Waals radii (3.7 Å) and, together with the overall asymmetry of the anion and its remarkable deviation from linearity, could be a consequence of charge-transfer or coulombic interactions taking place within the crystal.

In the structure of **3**, the three symmetry independent triiodide anions lie on crystallographic inversion centres. Two of them are in contact with the ligand tetrazine ring, both giving side-on interaction (Fig. 5a). Nevertheless, while one of them is very well placed above the ring centroid (I...ring centroid/offset distances 3.57/0.30 Å), the other one is more displaced toward the ring periphery (I...ring centroid/offset distances 3.61/0.80 Å). Interestingly, this second triiodide places its central iodine just above a C-N aromatic bond, so giving an η^2 -type binding. Differently from what found in the structure **2**, the crystallographic symmetry imposes both linearity and equal I-I bond distances to all anions (I-I bond distances in the three triiodides are 2.930, 2.933 and 2.937 Å). The anion...ring centroid distances in these adducts are very similar to those found in the crystal structures reported by Rissanen for I_3^- anion in complex with a pentafluorobenzylammonium and a N-(pentafluorobenzyl)pyridinium receptors.^{9a} Nevertheless, in the structures by Rissanen, the I_3^- anions are trapped in cavities, completely surrounded by the aromatic groups of the receptors, while in **2** and **3** there are segregate planes which contain only protonated ligands hydrogen-bonded to cocrystallized water molecules or only triiodide anions.

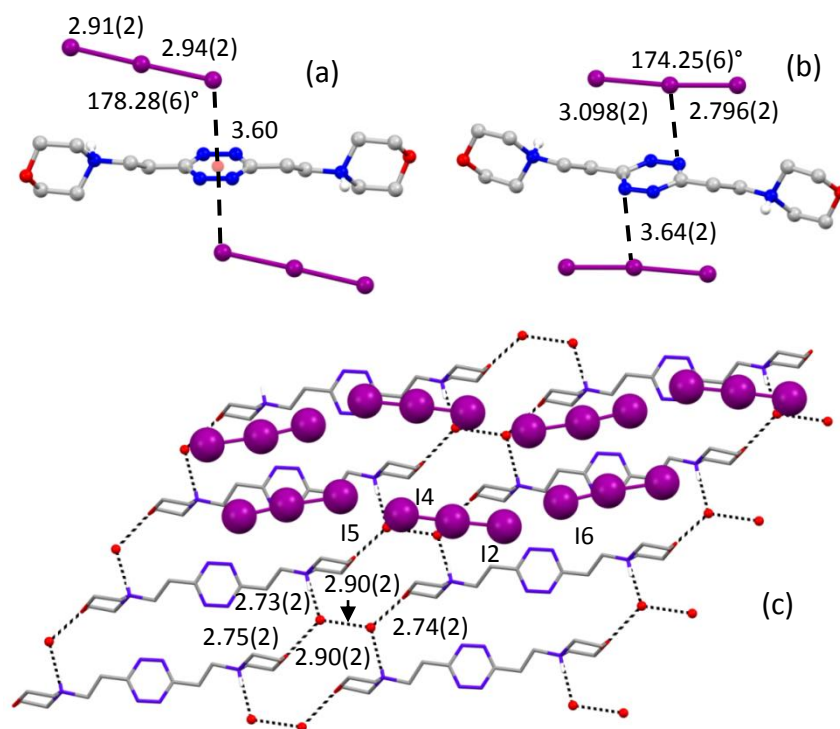


Fig. 4 Crystal structure of $\text{H}_2\text{L}_2(\text{I}_3)_2 \cdot 2\text{H}_2\text{O}$ (**2**): end-on (a) and side-on (b) $\text{I}_3^- \cdots \pi$ contacts; honeycomb-like network given by protonated ligands and co-crystallized water molecules and zig-zag chains of triiodide anions (c). Distances are in Å.

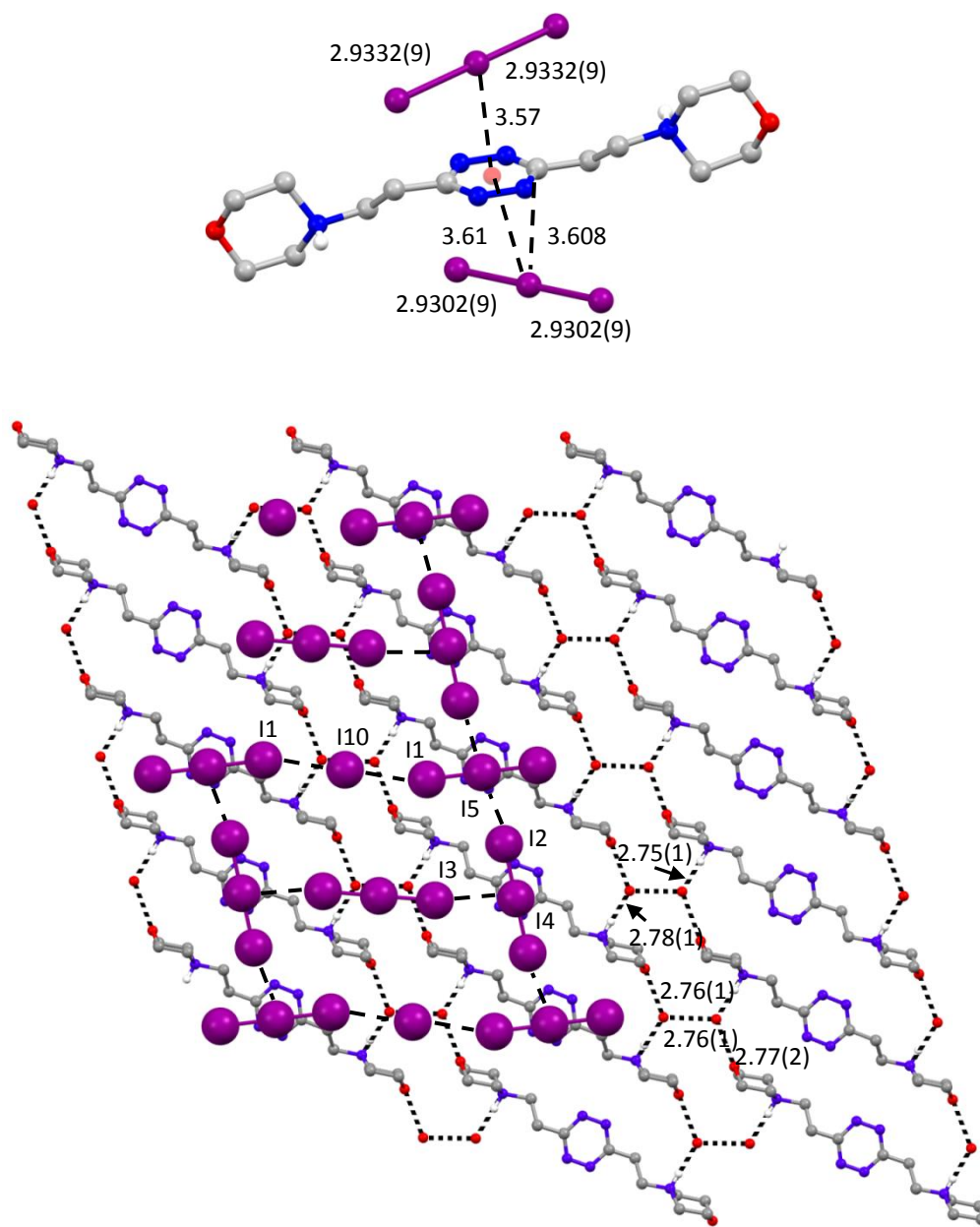


Fig. 5 Crystal structure of $(\text{H}_2\text{L}_2)_2(\text{I}_3)\cdot 4\text{H}_2\text{O}$ (**3**): ligand conformation and $\text{I}_3^- \cdots \pi$ contact (a); honeycomb-like network given by protonated ligands and co-crystallized water molecules and T-shaped pattern of triiodide anions (c). Distances are in Å.

Regarding the analogies of structures **2** and **3**, in both crystalline structures, the ligand assumes almost the same conformation, the protonated nitrogen atoms of the morpholine rings pointing toward opposite directions and establishing water assisted contacts with the oxygen atoms of adjacent ligands (Fig. 4c and 5b). Protonated ligands and cocrystallized water molecules define honeycomb-like networks developing parallel to the (100) planes both in **2** and **3**. The similarity between these two structures goes even further, since the tridimensional arrangement attained by the ligand molecules is practically the same in both of them, as evidenced by the graphical superimposition of the ligand components of the crystalline structure (Fig. S2[†]). Thus, the prime differences between structures **2** and **3** are the number

of iodine atoms and their arrangement into discrete anions, leading to different interhalogen contact networks in the anionic planar layers sandwiched between two successive planes of protonated ligands. Some contacts of the iodine anions with the aliphatic hydrogen atoms ($\text{H} \cdots \text{I}$ distances in the range 3.0–3.21 Å) contribute to stabilize the interplanar interaction. In particular, in **2**, parallel zig-zag chains are formed by the head-to-tail disposition of the anions (Fig. 4c). Interestingly, the $\text{I} \cdots \text{I}$ contacts in these chains ($\text{I}_2 \cdots \text{I}_6$ 3.530(2) and $\text{I}_4 \cdots \text{I}_5$ 3.578(2) Å) can be regarded as secondary bonds, being the van der Waals contacts about 3.8–3.9 Å.⁸ In the mixed I^-/I_3^- system **2**, iodide and triiodide anions alternate giving the T-shaped pattern shown in Fig. 5b. This structure

features longer I...I contacts ranging from 4.0230(9) to 4.3413(9) Å.

In view of the mechanisms currently accepted to interpret the conductivity showed by polyiodides¹¹⁻¹³ and the precedents of conductive crystalline structures containing such species,^{12a,24,41} it was reasoned that structure **2** and **3** are good candidates to show electrical conductivity by virtue of the segregation of the iodine anions in separate layers and their interconnections into infinite networks through I...I short contacts, thus the conductivity of the polyiodide complexes **2** and **3** are currently under evaluation.

Further information about geometries and structures of the different triiodide anions of **2** and **3** were acquired by the analysis of their Raman spectra (Fig. 6) in the frequency region below 250 cm⁻¹ which is characterized by vibrations involving the I₃⁻ units. In complex **3**, a single prominent band is observed at 110 cm⁻¹ (Fig. 6a), although, as shown by the inset in Fig. 6a, a lower intensity structure is present with weak shoulders at 60, 75 and a broad one at 154 cm⁻¹, respectively, and an additional very weak band at 221 cm⁻¹. Crystals of **2** show a more structured spectrum, where the main band centred at 112 cm⁻¹ is surrounded by few medium intensity peaks, indicating that I₃⁻ anions have lower symmetry than in the case of **3**.

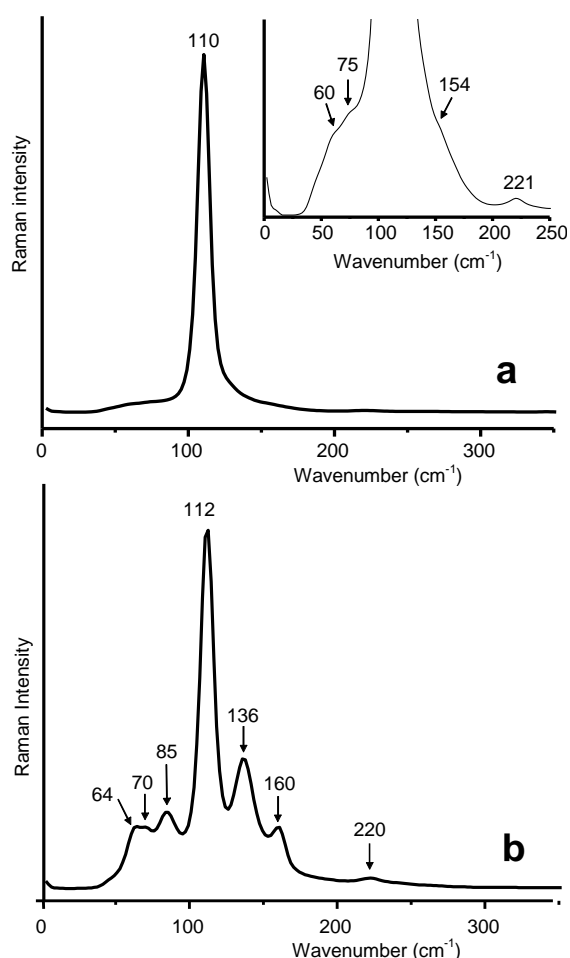


Fig. 6 Raman spectra of (H₂L₂)₂(I₃)₃I·4H₂O (a) and H₂L₂(I₃)₂·2H₂O (b).

In crystals of **3** ((H₂L₂)₂(I₃)₃I·4H₂O, Fig. 5), three kinds of I₃⁻ anions were identified, displaying linear and symmetric structures but with slightly different I-I bond lengths. For each anion, three vibrational modes are expected (one twofold), among which only the symmetric stretching is Raman active. Therefore, the intense band at 110 cm⁻¹ can be assigned to this vibration (ν₁). The presence of the very weak band at 221 cm⁻¹, assigned as 2ν₁, supports the linear structure of the ions.⁴² However, small deviations from linearity, when randomly occurring, can be compatible with an observed overall centrosymmetric lattice. In such a case, bending and asymmetric stretching would become Raman active, even though with very weak intensities. Most likely, the shoulders at about 75 cm⁻¹ and 154 cm⁻¹ have a similar origin and can be related to the bending (ν₂) and asymmetric stretching (ν₃), respectively.^{10j,43} The latter has been previously observed around 140-145 cm⁻¹.^{9g,10j,43,44} The difference with the present data may be ascribed to the difficulty in accurately locating the maximum position because of the convolution with the very intense ν₁.

The 60 cm⁻¹ shoulder can be attributed considering that, at room temperature, excited low frequency vibrational modes may be populated, hence also ν(1-2) vibrational transitions other than the fundamental ν(0-1) can be observed. For this reason, the 60 cm⁻¹ is probably a hot band transition of the bending vibration ν₂. Alternatively, it could be considered a lattice vibration (i.e. I₃⁻ with respect to the ligand),^{10j,43,45} but in our opinion 60 cm⁻¹ is a too high value for lattice modes.

As shown before, crystals of **2** (H₂L₂(I₃)₂·2H₂O, Fig. 4) contain two differently conformed I₃⁻ anions, (a) and (b), featuring end-on and side-on interaction modes, respectively, with the tetrazine ring. Both are non-linear, the bending angle of (b) being larger than that of (a). Moreover, the I-I distances are not symmetric with respect to the central atom and this is more evident in (b) than in (a), the latter being more similar to the symmetric I₃⁻ anions of complex **3**. Due to the loss of symmetry of (a) and (b), all three vibrational modes become Raman active accounting for the higher number of bands in the spectrum and for their increased intensities (Fig. 6, Table 3). Furthermore, the deviation from linearity of these anions causes a lowering of the force constant of bending vibrations, justifying, in the (a) case, the frequency shift toward lower energies (75/70 cm⁻¹; 145-140/136 cm⁻¹) observed for the relevant bands.

Table 3 Observed Raman frequencies of crystalline H₂L₂(I₃)₂·2H₂O [(a) and (b)] and (H₂L₂)₂(I₃)₃I·4H₂O (**3**) complexes

2 (a)	2 (b)	3	assignment
64 mw		60 vw	bending ν ₂ u(1-2)
70 w		75 vw	bending ν ₂ u(0-1)
112 s		110 vs	symmetric stretch ν ₁
136 ms		154 bs	asymmetric stretch ν ₃
220 w		221 vw	2ν ₁
	85 m		stretching I ₂ ...I
	160 m		stretching I-I...I

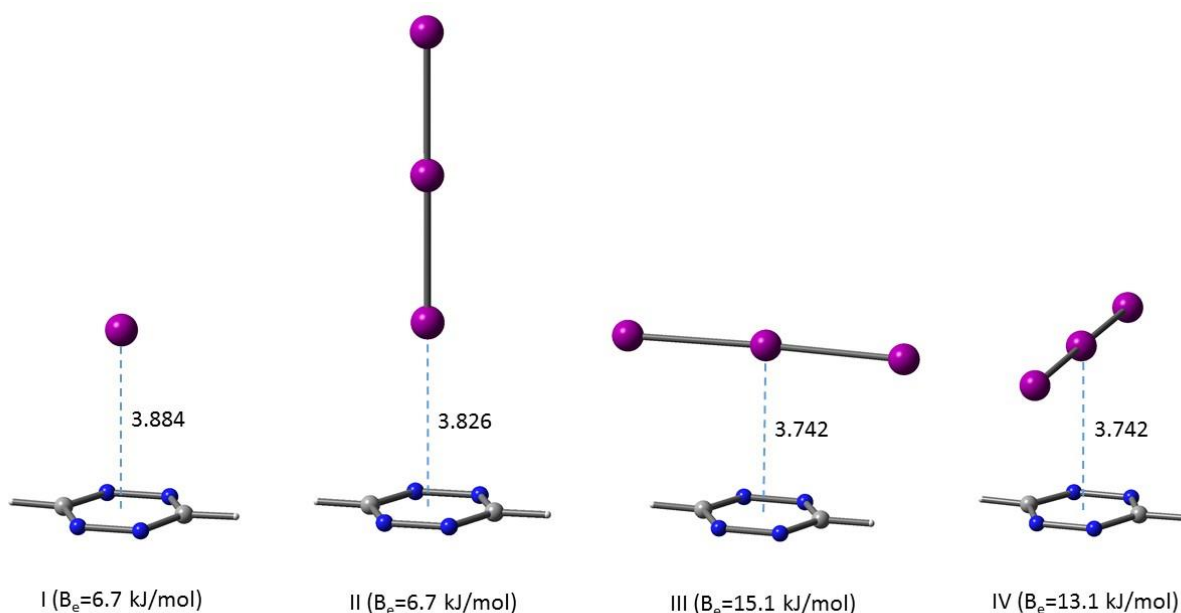


Fig. 7 DFT-optimized geometries of four tetrazine-anion complexes. Distances are in Å.

In (b), the I-I bond distances from the central iodine atom, although still below the limit reported for intramolecular distances in polyiodide systems (3.3 Å),^{8,46} are rather different, giving this triiodide anion some similarity with a $I_2 \cdots I^-$ system.^{98,47,48} This may help in the assignment of the 160 cm^{-1} and 85 cm^{-1} bands. Actually, the band at 160 cm^{-1} can be assigned to an I-I stretching “perturbed” by the presence of a close I^- ion, as already reported for systems with I-I distances comparable to (b),^{98,49} while the $I_2 \cdots I^-$ stretching should be found at lower frequency because of its longer bond distance (3.098 Å vs 2.796 Å, Fig. 4). The 85 cm^{-1} band can be attributed to this vibration. The bending is not observed, being likely hidden under this low frequency spectral feature.

In order to compare the relative strength of interaction of iodide and triiodide anions with the tetrazine moiety of L2, we investigated the four complexes shown in Fig. 7. Complex I is characterized by a binding energy (B_e) of 6.7 kJ/mol which results from the anion- π interaction

established between iodide and tetrazine with a $I^- \cdots$ centroid distance of 3.884 Å. Regarding the triiodide anion, three high-symmetry orientations above the molecular plane of tetrazine were conceived: one where I_3^- is oriented normal to the plane (complex II), a second one (complex III) where I_3^- is oriented parallel to the plane and aligned along the C-C axis, and a third one (complex IV) where the bond axis of I_3^- bisects the N-N bonds of tetrazine. Interestingly, complex III possesses both the lowest total electronic energy and the highest value of B_e (15.1 kJ/mol) among the triiodide complexes shown in Fig. 7. A rotation of the I_3^- anion about the (central I)-centroid axis by

90.0° yields complex IV which, in spite of having the same I-centroid distance of 3.742 Å of complex III, is characterized by a slightly lower B_e value (13.1 kJ/mol) with respect to the former. The most disfavoured orientation is the vertical one corresponding to complex II which is characterized by a B_e value (6.7 kJ/mol) that is same as that of the complex with iodide anion.

As far as the possibility of a charge transfer process is concerned, the results of our natural population analysis indicate that almost no charge is transferred from the anion to tetrazine. For instance, $q(I^-) = -0.99e$ in complex I while similar net charges were calculated for the complexes with triiodide anion. Interestingly, however, the negative charge accumulates on the terminal iodine

atoms of I_3^- while the charge of the central atom is close to zero. This results suggests that the terminal iodine atoms of I_3^- are likely favoured to interact electrostatically with the counter-cations both in solution and in the crystals. Nevertheless, it is to be underlined that the contacts found in our models are longer than the sum of the van der Waals radii and always significantly longer than those found at the solid state.

To unravel the nature of the intermolecular interactions that are operative within the I_3^- complexes both in the solid-state and in water, we have performed a topological analysis of the computed electronic charge density of the trimeric $(H_2L2^{2+})(I_3^-)_2$ complex displayed in Fig. 4b. The molecular graph obtained for the geometry corresponding to the crystal structure is

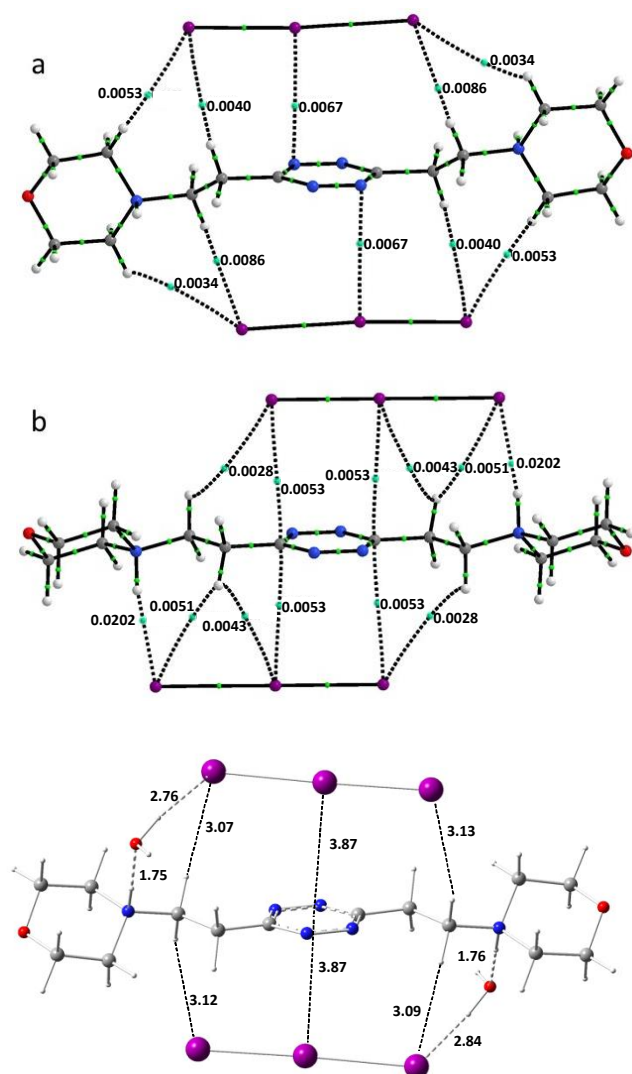


Fig. 8 Molecular graphs for (a) the $\text{H}_2\text{L}_2(\text{I}_3)_2$ complex in the molecular crystal and (b) the same complex after geometry optimization in a continuum water environment. The values of the charge density at selected BCP(3,-1) are reported (in a.u.) whereas RCPs and CCPs are not shown. (c) The same complex with two explicit water molecules. Distances are in Å.

concerned with C-H...I interactions and the fifth one with an N...I interaction. The latter is likely associated to an anion- π interaction rather than to halogen bonding interaction since it occurs in the direction normal to the tetrazine plane which is populated by π -electrons. The values of the electronic charge densities at the BCP(3,-1) indicates that the complex in the crystal is C_i symmetric. The binding energy associated to the interaction of two I_3^- anions with the dicationic ligand corresponds to 65.2 kJ/mol. Hence, half of this energy (32.6 kJ/mol) corresponds to the interaction of one I_3^- anion with the ligand. Upon replacement of both morpholinic arms with hydrogen atoms, the binding energy associated to the interaction of one I_3^- anion to the ligand becomes 10.2 kJ/mol, which approximately double the mean contribution from the four CH...I contacts. This value is slightly lower than those

shown in Fig. 8a. Each I_3^- anion interacts with the deprotonated ligand via five bond paths, four of which are calculated for complexes III and IV in Fig. 7. Hence, this result indicates that the parallel orientation of the I_3^- anion with respect to the tetrazine plane is still favoured over the vertical orientation (complex II) even when the triiodide anion is translated away from its centroid.

As above noted, we were not able to get information about I_3^- complexes in aqueous solution because they are poorly soluble. To remedy this lack of information, details of the possible geometry of the complex in water were obtained by optimization at the IEF-PCM(H_2O)- ω B97X-D/DGDZVP level of theory of the trimeric $(\text{H}_2\text{L}_2^{2+})(\text{I}_3^-)_2$ complex and of the same system solvated by two explicit water molecules. Both calculations were followed by QTAIM analysis of the electronic charge densities. The molecular graph of the DFT-optimized not solvated complex is shown in Fig. 8b. Each I_3^- anion is now characterized by six bond path connecting it to the diprotonated ligand. The new bond path topology results from the translation of the I_3^- anions in opposite directions, toward the positive ligand charges, nearly oriented along the C-C axis of the tetrazine ring. In addition to four C-H...I bond paths, each I_3^- anion is now characterized by two I...C bond paths connecting the central and one terminal iodine atoms of I_3^- with the carbon atoms of the tetrazine ring. The increased number of bonding interactions in this model is in line with the enhancement of the computed binding energy, by ~ 10 kcal/mol, from 15.58 kcal/mol to 25.25 kcal/mol. However, it is noteworthy that, in the solvated system (Fig. 8c), the charge assisted NH...I hydrogen bonds are lost and replaced by water bridged bonds, while the I... π and CH...I interactions still have a role in stabilizing the adduct.

Conclusions

The conclusions section should come in this section at the end of the article, before the acknowledgements. Protonated forms of the tetrazine-based ligand L2 are able to form I^+ , I_3^- , as well as mixed I^+/I_3^- anion complexes in the solid state. X-ray structures of these complexes showed that the anions are invariably located over the positive electrostatic potential of the ligand's tetrazine ring forming anion- π interactions. In the I^+ complex, further noncovalent forces contribute to hold the anions in place, while in the case of I_3^- solid complexes, constituted by alternated segregated planes containing only protonated ligands and cocrystallized water molecules or only iodide and triiodide anions forming halogen-halogen contacts, forces other than anion- π interactions appears to make a modest contribution to the anion-ligand association. In the solid complexes, the triiodide anion displays both end-on and side-on interaction modes with the tetrazine moieties, the I_3^- axis being aligned parallel to the ligand axis. DFT calculations substantiated that the side-on arrangement of I_3^- over the tetrazine ring corresponds to the most stable interaction mode among those computationally explored. Furthermore, calculations evidenced that, even when the ligand is deprived of the two morpholinium residues and in the presence of a

simulated implicit water environment, the tetrazine ring is still able to promote the association with I^- and I_3^- , the side-on orientation of I_3^- , relative to the aromatic ring, remaining the most stable conformation. The infinite two-dimensional networks established between I_3^- and I_3^-/I^- anions through $I\cdots I$ short contacts makes these crystalline structures good candidates to behave as solid conductors. While I_3^- complexes are of very low solubility, the I^- ones are soluble enough to allow the interaction of I^- with mono- and di-protonated forms of L2 to be studied. The stability of the complexes formed with HL_2^+ and $H_2L_2^{2+}$ are very similar, the free energy change of association ($-\Delta G^\circ$) being in the range 12–13 kJ/mol, in agreement with previous data²⁵ showing that anion association with L2 in aqueous solution is almost independent of ligand charge, suggesting that anion- π interactions prevails over electrostatic attraction. In the case of I_3^- , the formation of solution complexes was simulated by means of computational methods that showed the anion lying at short distance over the tetrazine ring and shifted toward a protonated morpholine nitrogen to form, this time, a salt-bridge interaction.

Acknowledgements

Financial support from the Italian MIUR (project 2015MP34H3) is gratefully acknowledged. The centre of instrumental facilities, STI, of the University of Jaén is acknowledged for technical assistance. FP thanks the Department of Applied Chemistry of the Graduate School of Engineering of Tohoku University for financial support.

Notes and references

- (a) K. Bowman-James, A. Bianchi and E. García-España, Eds., *Anion Coordination Chemistry*, Wiley-VCH, New York, 2012; (b) J. L. Sessler, P. A. Gale and W.-S. Cho, *Anion Receptor Chemistry (Monographs in Supramolecular Chemistry)*, RSC Publishing, Cambridge, 2006.
- D. Quiñero, A. Frontera and P. M. Deyà, in *Anion Coord. Chem.*, ed. E. Bowman-James, K., Bianchi, A., García-España, Wiley-VCH, New York, 2012, pp. 321–361.
- (a) M. Giese, M. Albrecht and K. Rissanen, *Chem. Commun.*, 2016, **52**, 1778–1795; (b) X. Lucas, A. Bauza, A. Frontera and D. Quiñero, *Chem. Sci.*, 2016, **7**, 1038–1050; (c) M. Giese, M. Albrecht and K. Rissanen, *Chem. Rev.*, 2015, **115**, 8867–8895; (d) S. E. Wheeler and J. W. G. Bloom, *J. Phys. Chem. A*, 2014, **118**, 6133–6147; (e) P. Gamez, *Inorg. Chem. Front.*, 2014, **1**, 35–43; (f) H. T. Chifotides and K. R. Dunbar, *Acc. Chem. Res.*, 2013, **46**, 894–906; (g) P. Ballester, *Acc. Chem. Res.*, 2013, **46**, 874–884; (h) M. M. Watt, M. S. Collins and D. W. Johnson, *Acc. Chem. Res.*, 2013, **46**, 955–966; (i) H.-J. Schneider, *Acc. Chem. Res.*, 2013, **46**, 1010–1019; (j) P. Arranz-Mascaros, C. Bazzicalupi, A. Bianchi, C. Giorgi, M.-L. Godino-Salido, M.-D. Gutierrez-Valero, R. Lopez-Garzon and M. Savastano, *J. Am. Chem. Soc.*, 2013, **135**, 102–105; (k) S. E. Wheeler, *Acc. Chem. Res.*, 2013, **46**, 1029–1038; (l) A. Frontera, P. Gamez, M. Mascal, T. J. Mooibroek and J. Reedijk, *Angew. Chemie, Int. Ed.*, 2011, **50**, 9564–9583; (m) L. M. Salonen, M. Ellermann and F. Diederich, *Angew. Chemie, Int. Ed.*, 2011, **50**, 4808–4842; (n) I. Alkorta, F. Blanco, P. M. Deyà, J. Elguero, C. Estarellas, A. Frontera and D. Quiñero, *Theor. Chem. Acc.*, 2010, **126**, 1–14; (o) O. B. Berryman and D. W. Johnson, *Chem. Commun.*, 2009, 3143–3153; (p) C. Caltagirone and P. A. Gale, *Chem. Soc. Rev.*, 2009, **38**, 520–563; (q) H.-J. Schneider, *Angew. Chemie, Int. Ed.*, 2009, **48**, 3924–3977; (r) B. L. Schottel, H. T. Chifotides and K. R. Dunbar, *Chem. Soc. Rev.*, 2008, **37**, 68–83; (s) B. P. Hay and V. S. Bryantsev, *Chem. Commun.*, 2008, 2417–2428; (t) D. Quiñero, C. Garau, C. Rotger, A. Frontera, P. Ballester, A. Costa and P. M. Deyà, *Angew. Chemie, Int. Ed.*, 2002, **41**, 3389–3392; (u) M. Mascal, A. Armstrong and M. D. Bartberger, *J. Am. Chem. Soc.*, 2002, **124**, 6274–6276; (v) I. Alkorta, I. Rozas and J. Elguero, *J. Am. Chem. Soc.*, 2002, **124**, 8593–8598; (w) K. Hiraoka, S. Mizuse and S. Yamabe, *J. Phys. Chem.*, 1987, **91**, 5294–5297.
- (a) Z. Aliakbar Tehrani and K. S. Kim, *Int. J. Quantum Chem.*, 2016, **116**, 622–633; (b) J.-Z. Liao, H.-L. Zhang, S.-S. Wang, J.-P. Yong, X.-Y. Wu, R. Yu and C.-Z. Lu, *Inorg. Chem.*, 2015, **54**, 4345–4350; (c) M. Savastano, P. Arranz-Mascaros, C. Bazzicalupi, A. Bianchi, C. Giorgi, M. L. Godino-Salido, M. D. Gutierrez-Valero and R. López-Garzón, *RSC Adv.*, 2014, **4**, 58505–58513; (d) P. Arranz, A. Bianchi, R. Cuesta, C. Giorgi, M. L. Godino, M. D. Gutierrez, R. Lopez and A. Santiago, *Inorg. Chem.*, 2010, **49**, 9321–9332; *Inorg. Chem.*, 2012, **51**, 4883.
- (a) P. A. Gale and C. Caltagirone, *Chem. Soc. Rev.*, 2015, **44**, 4212–4227; (b) N. H. Evans and P. D. Beer, *Angew. Chemie, Int. Ed.*, 2014, **53**, 11716–11754.
- (a) A. Vargas Jentzsch and S. Matile, *Top. Curr. Chem.*, 2015, **358**, 205–239; (b) A. Vargas Jentzsch and S. Matile, *J. Am. Chem. Soc.*, 2013, **135**, 5302–5303; (c) A. Vargas Jentzsch, A. Hennig, J. Mareda and S. Matile, *Acc. Chem. Res.*, 2013, **46**, 2791–2800; (d) A. V. Jentzsch, D. Emery, J. Mareda, S. K. Nayak, P. Metrangolo, G. Resnati, N. Sakai and S. Matile, *Nat. Commun.*, 2012, **3**, 905; (e) J. Misek, A. V. Jentzsch, S. Sakurai, D. Emery, J. Mareda and S. Matile, *Angew. Chemie, Int. Ed.*, 2010, **49**, 7680–7683; (f) L. Adriaenssens, C. Estarellas, A. Vargas Jentzsch, M. Martínez Belmonte, S. Matile and P. Ballester, *J. Am. Chem. Soc.*, 2013, **135**, 8324–8330; (g) A. Vargas Jentzsch, D. Emery, J. Mareda, P. Metrangolo, G. Resnati and S. Matile, *Angew. Chemie, Int. Ed.*, 2011, **50**, 11675–11678.
- (a) Y. Zhao, S. Benz, N. Sakai and S. Matile, *Chem. Sci.*, 2015, **6**, 6219–6223; (b) Y. Zhao, N. Sakai and S. Matile, *Nat. Commun.*, 2014, **5**, 3911; (c) Y. Zhao, C. Beuchat, Y. Domoto, J. Gajewy, A. Wilson, J. Mareda, N. Sakai and S. Matile, *J. Am. Chem. Soc.*, 2014, **136**, 2101–2111; (d) T. Lu and S. E. Wheeler, *Org. Lett.*, 2014, **16**, 3268–3271; (e) C. Estarellas, A. Frontera, D. Quiñero and P. M. Deyà, *Angew. Chemie, Int. Ed.*, 2011, **50**, 415–418; (f) C. M. Rojas and J. J. Rebeck, *J. Am. Chem. Soc.*, 1998, **120**, 5120–5121.
- P. H. Svensson and L. Kloo, *Chem. Rev.*, 2003, **103**, 1649–1684.
- (a) M. Giese, M. Albrecht, T. Repenko, J. Sackmann, A. Valkonen and K. Rissanen, *European J. Org. Chem.*, 2014, **2014**, 2435–2442; (b) M. D. Garcia, J. Marti-Rujas, P. Metrangolo, C. Peinador, T. Pilati, G. Resnati, G. Terraneo and M. Ursini, *CrystEngComm*, 2011, **13**, 4411–4416; (c) M. Müller, M. Albrecht, V. Gossen, T. Peters, A. Hoffmann, G. Raabe, A. Valkonen and K. Rissanen, *Chem. - A Eur. J.*, 2010, **16**, 12446–12453, S12446/1–S12446/4; (d) H. Chow, P. A. W. Dean, D. C. Craig, N. T. Lucas, M. L. Scudder and I. G. Dance, *New J. Chem.*, 2003, **27**, 704–713; (e) H. Paulsson, M. Berggrund, A. Fischer and L. Kloo, *Eur. J. Inorg. Chem.*, 2003, 2352–2355; (f) A. J. Blake, R. O. Gould, W.-S. Li, V. Lippolis, S. Parsons, C. Radek and M. Schroder, *Angew. Chemie, Int. Ed.*, 1998, **37**, 293–296; (g) A. J. Blake, W.-S. Li, V. Lippolis, M. Schroder, F. A. Devillanova, R. O. Gould, S. Parsons and C. Radek, *Chem. Soc. Rev.*, 1998, **27**, 195–206; (h) A. J. Blake, V. Lippolis, S. Parsons and M. Schroeder, *Chem. Commun.*, 1996,

- 2207–2208; (i) R. D. Bailey and W. T. Pennington, *Chem. Commun.*, 1998, 1181–1182; (j) A. J. Blake, R. O. Gould, S. Parsons, C. Radek and M. Schroeder, *Angew. Chemie, Int. Ed. English*, 1995, **34**, 2374–2376.
- 10 (a) K. Lamberts, P. Handels, U. Englert, E. Aubert and E. Espinosa, *CrystEngComm*, 2016, **18**, 3832–3841; (b) D. Tristant, P. Puech and I. C. Gerber, *Phys. Chem. Chem. Phys.*, 2015, **17**, 30045–30051; (c) Y. Wang, Y. Xue, X. Wang, Z. Cui and L. Wang, *J. Mol. Struct.*, 2014, **1074**, 231–239; (d) R. D. Walsh, J. M. Smith, T. W. Hanks and W. T. Pennington, *Cryst. Growth Des.*, 2012, **12**, 2759–2768; (e) G. Manca, A. Ienco and C. Mealli, *Cryst. Growth Des.*, 2012, **12**, 1762–1771; (f) M. Otsuka, H. Mori, H. Kikuchi and K. Takano, *Comput. Theor. Chem.*, 2011, **973**, 69–75; (g) M. Groessel, Z. Fei, P. J. Dyson, S. A. Katsyuba, K. L. Vikse and J. S. McIndoe, *Inorg. Chem.*, 2011, **50**, 9728–9733; (h) A. Asaduzzaman and G. Schreckenbach, *Theor. Chem. Acc.*, 2009, **122**, 119–125; (i) V. T. Calabrese and A. Khan, *J. Phys. Chem. A*, 2000, **104**, 1287–1292; (j) P. H. Svensson and L. Kloo, *J. Chem. Soc. Dalt. Trans. Inorg. Chem.*, 2000, 2449–2455; (k) S. B. Sharp and G. I. Gellene, *J. Phys. Chem. A*, 1997, **101**, 2192–2197; (l) G. A. Landrum, N. Goldberg and R. Hoffmann, *J. Chem. Soc. Dalt. Trans. Inorg. Chem.*, 1997, 3605–3613.
- 11 C. L. Bentley, A. M. Bond, A. F. Hollenkamp, P. J. Mahon and J. Zhang, *J. Phys. Chem. C*, 2014, **118**, 22439–22449.
- 12 R. Thapa and N. Park, *J. Phys. Chem. Lett.*, 2012, **3**, 3065–3069.
- 13 W. Yourey, L. Weinstein and G. G. Amatucci, *Solid State Ionics*, 2011, **204**, 80–86.
- 14 (a) J. Wu, Z. Lan, J. Lin, M. Huang, Y. Huang, L. Fan and G. Luo, *Chem. Rev.*, 2015, **115**, 2136–2173; (b) A. Hagfeldt, G. Boschloo, L. Sun, L. Kloo and H. Pettersson, *Chem. Rev.*, 2010, **110**, 6595–6663; (c) M. Grätzel, *Chem. Lett.*, 2005, **34**, 8–13; (d) M. Grätzel, *Nat.*, 2001, **414**, 338–344.
- 15 M. Yu, W. D. McCulloch, Z. Huang, B. B. Trang, J. Lu, K. Amine and Y. Wu, *J. Mater. Chem. A*, 2016, **4**, 2766–2782.
- 16 F. Bella, S. Galliano, M. Falco, G. Viscardi, C. Barolo, M. Gratzel and C. Gerbaldi, *Chem. Sci.*, 2016, **7**, 4880–4890.
- 17 F. Bella, C. Gerbaldi, C. Barolo and M. Gratzel, *Chem. Soc. Rev.*, 2015, **44**, 3431–3473.
- 18 (a) Z. Fei, F. D. Bobbink, E. Păunescu, R. Scopelliti and P. J. Dyson, *Inorg. Chem.*, 2015, **54**, 10504–10512; (b) H.-C. Chang, J.-C. Jiang, M.-H. Kuo, D.-T. Hsu and S. H. Lin, *Phys. Chem. Chem. Phys.*, 2015, **17**, 21143–21148; (c) H. Santa-Nokki, S. Busi, J. Kallioinen, M. Lahtinen and J. Korppi-Tommola, *J. Photochem. Photobiol. A Chem.*, 2007, **186**, 29–33; (d) R. Kawano and M. Watanabe, *Chem. Commun.*, 2005, 2107–2109.
- 19 E. Yilmaz, E. B. Olutas, G. Barim, J. Bandara and O. Dag, *RSC Adv.*, 2016, **6**, 97430–97437.
- 20 P. E. Marchezi, G. G. Sonai, M. K. Hirata, M. A. Schiavon and A. F. Nogueira, *J. Phys. Chem. C*, 2016, **120**, 23368–23376.
- 21 K. Prabakaran, A. K. Palai, S. Mohanty and S. K. Nayak, *RSC Adv.*, 2015, **5**, 66563–66574.
- 22 J. Li and Z.-S. Wang, *RSC Adv.*, 2015, **5**, 56967–56973.
- 23 H. Wang, J. Li, F. Gong, G. Zhou and Z.-S. Wang, *J. Am. Chem. Soc.*, 2013, **135**, 12627–12633.
- 24 H. Wang, H. Li, B. Xue, Z. Wang, Q. Meng and L. Chen, *J. Am. Chem. Soc.*, 2005, **127**, 6394–6401.
- 25 M. Savastano, C. Bazzicalupi, C. Giorgi, C. García-Gallarín, M. D. López de la Torre, F. Pichierrri, A. Bianchi and M. Melguizo, *Inorg. Chem.*, 2016, **55**, 8013–8024.
- 26 C. Bazzicalupi, A. Bianchi, C. Giorgi, P. Gratteri, P. Mariani and B. Valtancoli, *Inorg. Chem.*, 2013, **52**, 2125–2137.
- 27 P. Gans, A. Sabatini and A. Vacca, *Talanta*, 1996, **43**, 1739–1753.
- 28 Agilent, *CrysAlis PRO (Version 1.171.35.11)*, Agilent Technologies Ltd, Yarnton, Oxfordshire, England, 2014.
- 29 G. M. Sheldrick, *Acta Crystallogr. Sect. A Found. Crystallogr.*, 1990, **A46**, 467–473.
- 30 G. M. Sheldrick, *Acta Crystallogr. Sect. C Struct. Chem.*, 2015, **71**, 3–8.
- 31 M. J. Frisch, G. W. Trucks, H. B. Schlegel, G. E. Scuseria, M. A. Robb, J. R. Cheeseman, G. Scalmani, V. Barone, B. Mennucci, G. A. Petersson, H. Nakatsuji, M. Caricato, X. Li, H. P. Hratchian, A. F. Izmaylov, J. Bloino, G. Zheng, J. L. Sonnenberg, M. Hada, M. Ehara, K. Toyota, R. Fukuda, J. Hasegawa, M. Ishida, T. Nakajima, Y. Honda, O. Kitao, H. Nakai, T. Vreven, J. A. Montgomery, J. E. Peralta, F. Ogliaro, M. Bearpark, J. J. Heyd, K. N. Kundin, V. N. Staroverov, R. Kobayashi, J. Normand, K. Raghavachari, A. Rendell, J. C. Burant, S. S. Iyengar, J. Tomasi, M. Cossi, N. Rega, J. M. Millam, M. Klene, J. E. Knox, J. B. Cross, V. Bakken, C. Adamo, J. Jaramillo, R. Gomperts, R. E. Stratmann, O. Yazyev, A. J. Austin, R. Cammi, C. Pomelli, J. W. Ochterski, R. L. Martin, K. Morokuma, V. G. Zakrzewski, G. A. Voth, P. Salvador, J. J. Dannenberg, S. Dapprich, A. D. Daniels, Ö. Farkas, J. B. Foresman, J. V. Ortiz, J. Ciolowski and D. J. Fox, *Gaussian 09, Revision C.01*, Gaussian, Inc., Wallingford CT, 2009.
- 32 J.-D. Chai and M. Head-Gordon, *Phys. Chem. Chem. Phys.*, 2008, **10**, 6615–6620.
- 33 N. Godbout, D. R. Salahub, J. Andzelm and E. Wimmer, *Can. J. Chem.*, 1992, **70**, 560–571.
- 34 C. Sosa, J. Andzelm, B. C. Elkin, E. Wimmer, K. D. Dobbs and D. A. Dixon, *J. Phys. Chem.*, 1992, **96**, 6630–6636.
- 35 J. Tomasi, B. Mennucci and R. Cammi, *Chem. Rev.*, 2005, **105**, 2999–3093.
- 36 S. F. Boys and F. Bernardi, *Mol. Phys.*, 1970, **19**, 553–566.
- 37 A. E. Reed, L. A. Curtiss and F. Weinhold, *Chem. Rev.*, 1988, **88**, 899–926.
- 38 T. A. Keith, *AIMA11 (Version 12.06.03, Professional)*, 2012.
- 39 F. W. Bader, *Atoms in Molecules: A Quantum Theory.*, Oxford Univ. Press, Oxford, 1994.
- 40 (a) P. Mateus, N. Bernier and R. Delgado, *Coord. Chem. Rev.*, 2010, **254**, 1726–1747; (b) K. Bowman-James, *Acc. Chem. Res.*, 2005, **38**, 671–678; (c) E. Garcia-España, P. Díaz, J. M. Llinares and A. Bianchi, *Coord. Chem. Rev.*, 2006, **250**, 2952–2986; (d) A. Bianchi, M. Micheloni and P. Paoletti, *Inorganica Chim. Acta*, 1988, **151**, 269–272.
- 41 Madhu, H. A. Evans, V. V. T. Doan-Nguyen, J. G. Labram, G. Wu, M. L. Chabinyr, R. Seshadri and F. Wudl, *Angew. Chemie Int. Ed.*, 2016, **55**, 8032–8035.
- 42 R. Swietlik, D. Schweitzer and H. J. Keller, *Phys. Rev. B Condens. Matter Mater. Phys.*, 1987, **36**, 6881–6888.
- 43 L. Kloo, P. H. Svensson and M. J. Taylor, *J. Chem. Soc. Dalt. Trans. Inorg. Chem.*, 2000, 1061–1065.
- 44 P. Deplano, F. A. Devillanova, J. R. Ferraro, F. Isaia, V. Lippolis and M. L. Mercuri, *Appl. Spectrosc.*, 1992, **46**, 1625–1629.
- 45 J. S. Zambounis, E. I. Kamitsos, A. P. Patsis and G. C. Papavassiliou, *J. Raman Spectrosc.*, 1992, **23**, 81–85.
- 46 P. Coppens, in *Ext. Linear Chain Compd.*, Plenum, 1982, vol. 1, pp. 333–356.
- 47 F. Bigoli, P. Deplano, F. A. Devillanova, V. Lippolis, M. L. Mercuri, M. A. Pellinghelli and E. F. Trogu, *Inorganica Chim. Acta*, 1998, **267**, 115–121.
- 48 L. Kloo, J. Rosdahl and P. H. Svensson, *Eur. J. Inorg. Chem.*, 2002, 1203–1209.
- 49 F. Groenewald, C. Esterhuysen and J. Dillen, *Theor. Chem. Acc.*, 2012, **131**, 1–12.